Sensor and Simulation Notes

Note XXXV 35

December 1966

Electromagnetic Fields from a Finite Line-Current Element

W. E. Blair

Stanford Research Institute
Menlo Park, California

Abstract

The transmitted electromagnetic fields from a thin vertical monopole over a reasonably flat earth are computed for any point in space. The theoretical model is a finite line-current element of sinusoidal distribution oriented vertically over a perfectly conducting flat earth. The assumptions of a sinusoidal current distribution and a perfect earth are reasonable for radio frequencies below 10 MHz.

The nonzero field components (E_z, E_ρ, H_φ) in cylindrical coordinates are computed from closed-form solutions and plotted for various combinations of antenna length, radial and vertical position of the observer, and transmitting frequency. The results indicate distinct differences between the current distribution and a point source. The conclusion is that, within a distance of two antenna lengths of the antenna, the infinitesimal dipole fields can differ considerably from the distributed dipole fields regardless of the electrical length of the antenna. Consequently, the distributed source must be used to compute reasonably correct fields within a distance of two antenna lengths from the antenna.

PL/PA 10/27/94

PL 94-0906

I. Introduction.

The fields everywhere outside of a vertical thin-monopole transmitting antenna over a reasonably flat earth can be determined analytically under reasonably ideal circumstances. A transmitting thin monopole (one whose length is much larger than the cross-section radius) can be replaced by a finite line-current distribution for most radio frequencies. For frequencies below approximately 10 MHz, the earth is a much better conductor than it is a dielectric, so the reasonably flat earth can be replaced by a flat, perfectly conducting ground plane. The transmitter coupler can be replaced by an infinitesimal source gap under normal circumstances.

By using this model, the ground plane can be replaced by the mirror image, thus creating a symmetrical dipole model and a symmetrical line-current distribution, which are convenient for analysis. This model is most easily described in a cylindrical coordinate system.

II. Current Distribution Model.

The line-current geometry and coordinate system are shown in figure 1. The thin, cylindrical monopole antenna of height ℓ and equivalent radius a is replaced by a line-current distribution of length ℓ. The current element is a function of height z and is positioned at $\rho = 0$ in a cylindrical coordinate system. The ideal, infinitesimal source is positioned on the ground (perfect image plane) at the origin of the coordinate system.

The line-current element is assumed, ideally, to be centered on the axis of the antenna. If the antenna has a polygonal cross section, it can be represented by an effective or equivalent circular cross section (Lo, 1953). The ideal line-current element passes through the center of this equivalent circle. The functional form of the line current on a cylindrical antenna is approximated by the following sinusoidal distribution (King, 1956):

$$I\,(z) \;=\; I_o \sin\left[k(\ell - |z|)\right], \quad \rho = 0 \;, \tag{1}$$

where

I_o = peak value of current (amperes)

ℓ = antenna (current-element) length (meters)

k = $\omega/c \;=\; 2\pi/\lambda$, the propagation constant (meters^{-1})

ω = $2\pi f$, the radian frequency (seconds^{-1})

f = frequency (hertz)

λ = wavelength (meters).

This current approximation is correct within a few percent for most cases, and it permits calculation of closed-form solutions. An extremely accurate line-current distribution is available (King and Wu, 1965), however, if one is willing to use numerical integration techniques to evaluate the solution integrals.

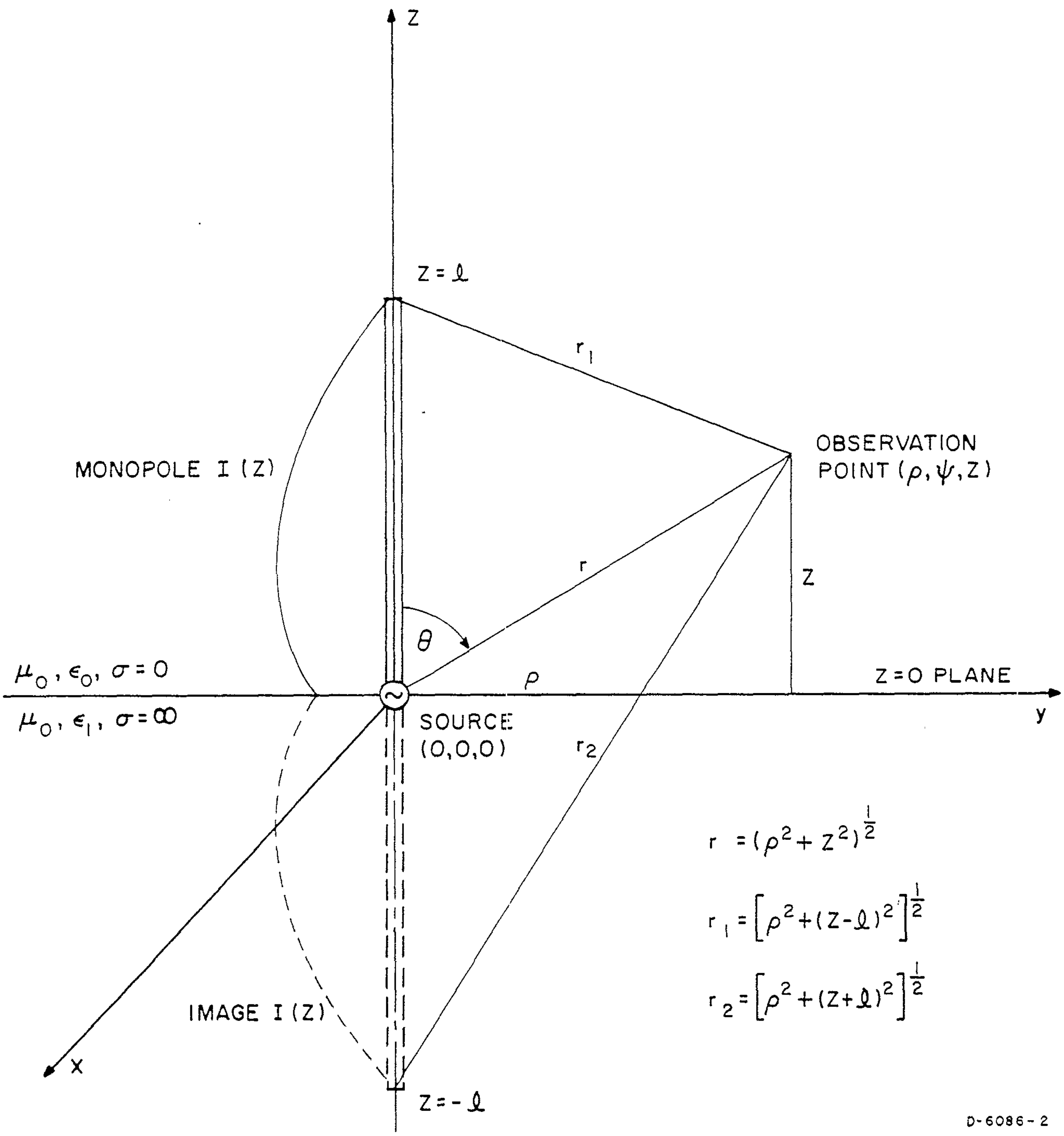

FIG. 1 IDEAL VERTICAL MONOPOLE AND IMAGE COORDINATE SYSTEM

III. Electromagnetic Fields: Formulation.

The electromagnetic field components of the sinusoidal line-current element have been computed in closed form (Jordan, 1950) by using the vector potential $\vec{A}$, in Maxwell's equations. The vector potential $\vec{A}$ for the current distribution given in equation (1) contains a component only in the z-direction, is a function only of ρ, and is

$$\vec{A} = A_z u_z = \frac{I_o}{4\pi}\left[\int_o^{\ell} \sin k(\ell - z)\ \frac{e^{-jkr}}{r}\ dz + \int_{-\ell}^{o} \sin k(\ell + z)\ \frac{e^{-jkr}}{r}\ dz\right] u_z \ , \qquad (2)$$

where $r = \left(\rho^2 + z^2\right)^{\frac{1}{2}}$.

u = unit vector

By using an exponential representation of the sinusoidal functions,

$$\sin\left[k(\ell \pm z)\right] = \frac{e^{jk(\ell \pm z)} - e^{-jk(\ell \pm z)}}{2} \ , \qquad (3)$$

equation (2) can be written as a collection of exponential integrals.

The magnetic field $\vec{H}$, as defined from the vector potential, is

$$\vec{H} = \nabla \times \vec{A} \ , \qquad (4)$$

which in cylindrical coordinates gives simply

$$H_\varphi = - \frac{\partial A_z}{\partial \rho} \qquad (5)$$

Substituting equation (3) into equation (2) and then into equation (5) gives the φ-component (the only component) of the magnetic field as a collection of four integrals whose integrands are, fortunately, perfect differentials. Hence these integrals are easily written in closed form. Having the magnetic field vector, one obtains the electric field $\vec{E}$, or displacement $\vec{D}$, directly from Maxwell's equation:

$$\frac{\partial \vec{D}}{\partial t} = \epsilon_o \frac{\partial \vec{E}}{\partial t} = \nabla \times \vec{H} \qquad (6)$$

where ϵ_o is the permittivity of free space. For a monochromatic radian frequency ω, then, the electric field is simply

$$\vec{E} = \frac{\nabla \times \vec{H}}{j\omega\epsilon_o} \quad , \tag{7}$$

where the monochromatic time factor $e^{+j\omega t}$ is understood.

By using equations (2) through (7), it can be shown (Jordan, 1950) that the nonzero field components (vertical electric E_z, radial electric E_ρ, and azimuthal magnetic H_φ) are written in closed form. The other field components (azimuthal electric E_φ, vertical magnetic H_z, and radial magnetic H_ρ) are theoretically zero. The fields are normalized to the product of the terminal voltage V_t and the terminal capacitance C_t, assuming terminal impedance Z_t, defined by

$$I_t = \frac{V_t}{Z_t} = j\omega C_t V_t \quad . \tag{8}$$

The normalized fields are summarized as follows:

$$\frac{E_z}{V_t C_t} = \frac{k}{4\pi\epsilon_o} \left[G_2 + G_1 - 2(\cos k\ell)\ G \right] \tag{9}$$

$$\frac{E_\rho}{V_t C_t} = \frac{-k}{4\pi\epsilon_o \rho} \left[(z + \ell)\ G_2 + (z - \ell)\ G_1 - 2z(\cos k\ell)\ G \right] \tag{9b}$$

$$\frac{H_\varphi}{V_t C_t} = \frac{-f}{2\rho} \left[r_2 G_2 + r_1 G_1 - 2(\cos k\ell)\ rG \right] \quad , \tag{9c}$$

where $$G = e^{-jkr}/r \tag{9d}$$

$$G_1 = e^{-jkr_1}/r_1 \tag{9e}$$

$$G_2 = e^{-jkr_2}/r_2 \tag{9f}$$

$$r = \left(\rho^2 + z^2 \right)^{\frac{1}{2}} \tag{9g}$$

$$r_1 = \left[\rho^2 + (z - \ell)^2 \right]^{\frac{1}{2}} \tag{9h}$$

$$r_2 = \left[\rho^2 + (z + \ell)^2 \right]^{\frac{1}{2}} \tag{9i}$$

and $e^{+j\omega t}$ is understood.

The electric and magnetic field equations (9) give the nonzero field components everywhere for $z \geq 0$, $\rho = 0$, as functions of (z, ρ). All of the field components are independent of φ. It is interesting to observe that the solutions are a remarkably simple closed-form collection of variations of the generalized Green's function, $e^{j(\omega t - kr)}/r$.

For completeness, the corresponding equations for an electric dipole point source are included as follows (Jordan, 1950):

$$\frac{E_z}{V_t C_t} = -\frac{(\Delta\ell)k^2}{4\pi\epsilon_o}\left[1 - \frac{j}{kr} - \frac{1}{(kr)^2}\right] G \sin\theta \tag{10a}$$

$$\frac{E_r}{V_t C_t} = +j\,\frac{(\Delta\ell)k}{2\pi\epsilon_o}\left(1 - \frac{j}{kr}\right)\frac{G}{r}\cos\theta \tag{10b}$$

$$\frac{H_\varphi}{V_t C_t} = -\frac{(\Delta\ell)k^2}{4\pi\epsilon_o}\left(1 - \frac{j}{kr}\right)\cdot G \sin\theta \tag{10c}$$

where $\Delta\ell$ is the infinitesimal dipole length. The dipole moment in equation (10) is $M = I_t \Delta\ell$ and with equation (8) can be written as $M = j\omega C_t V_t \Delta\ell$.

IV. Electromagnetic Fields: Computation and Graphs.

The three nonzero electromagnetic field components E_z, E_ρ, and H_φ given by equation (9) are computed and plotted for various combinations of parameters. All the field components are functions of position (ρ, z), monopole length ℓ, and transmitter frequency f. The component $E_\rho \equiv 0$ for $z = 0$. Since each of these three components is generally a complex quantity, the magnitude of each component is plotted. The magnitudes of components E_z and H_φ are plotted as functions of ρ in figure 2 for $z = 0$, for monopole length $\ell = 33$m, and for the frequencies f = 0.51 MHz, 2.4 MHz (quarter wavelength), and 7.0 MHz (three-quarter wavelength). The components E_z, and E_ρ, and H_φ are plotted as functions of ρ for the same three frequencies in figures 3 and 4 for a fixed height of z = 9.15m and in figures 5 and 6 for z = 18.3m. The components E_z, E_ρ, and H_φ are plotted as functions of z for the same three frequencies in figures 7 and 8 for a fixed radial position of $\rho = 20.3$m and in figures 9 and 10 for $\rho = 40.6$m.

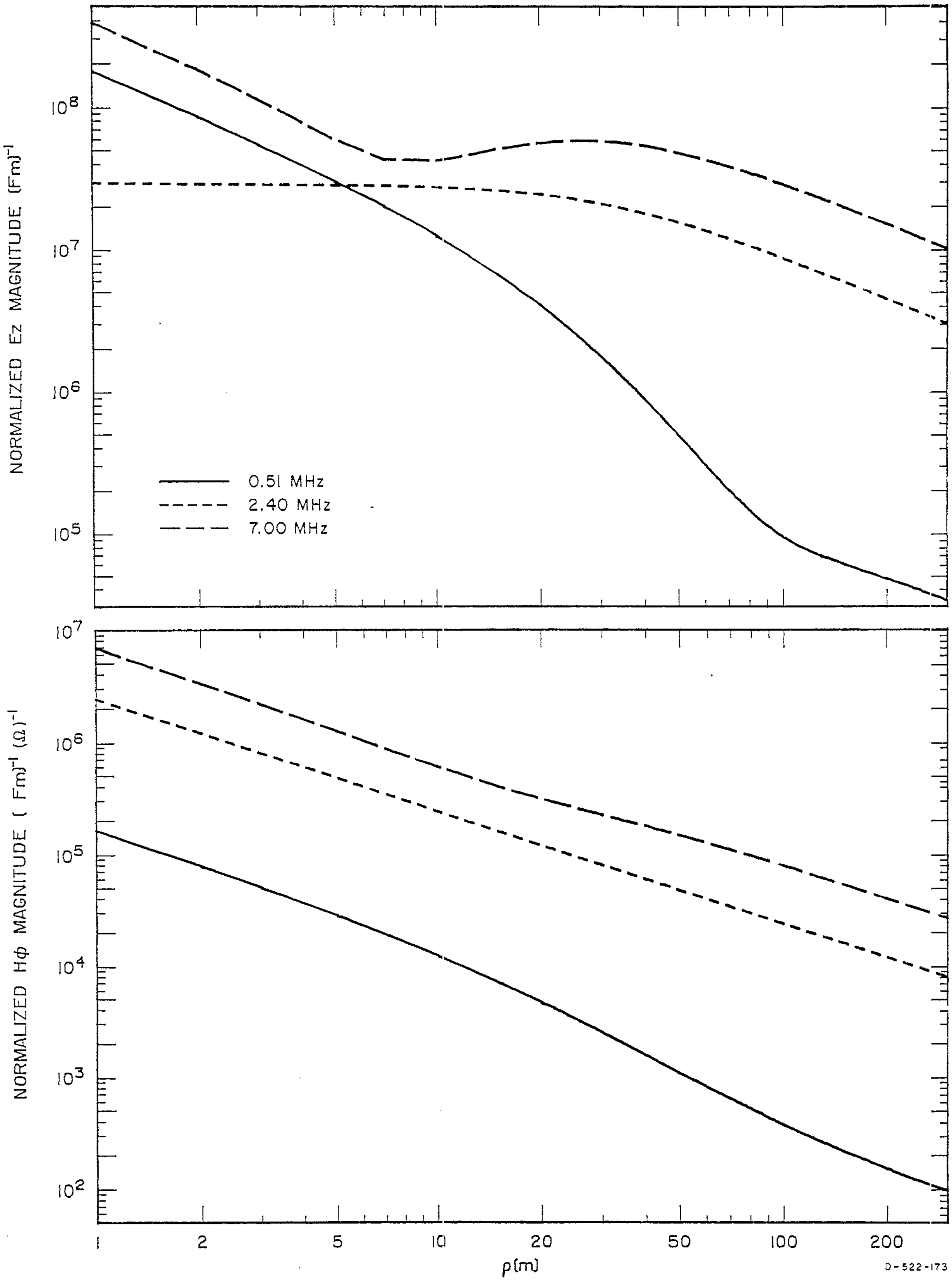

FIG. 2 NORMALIZED ELECTRIC AND MAGNETIC FIELD COMPONENTS FOR $z = 0$, $\ell = 33.1$ m

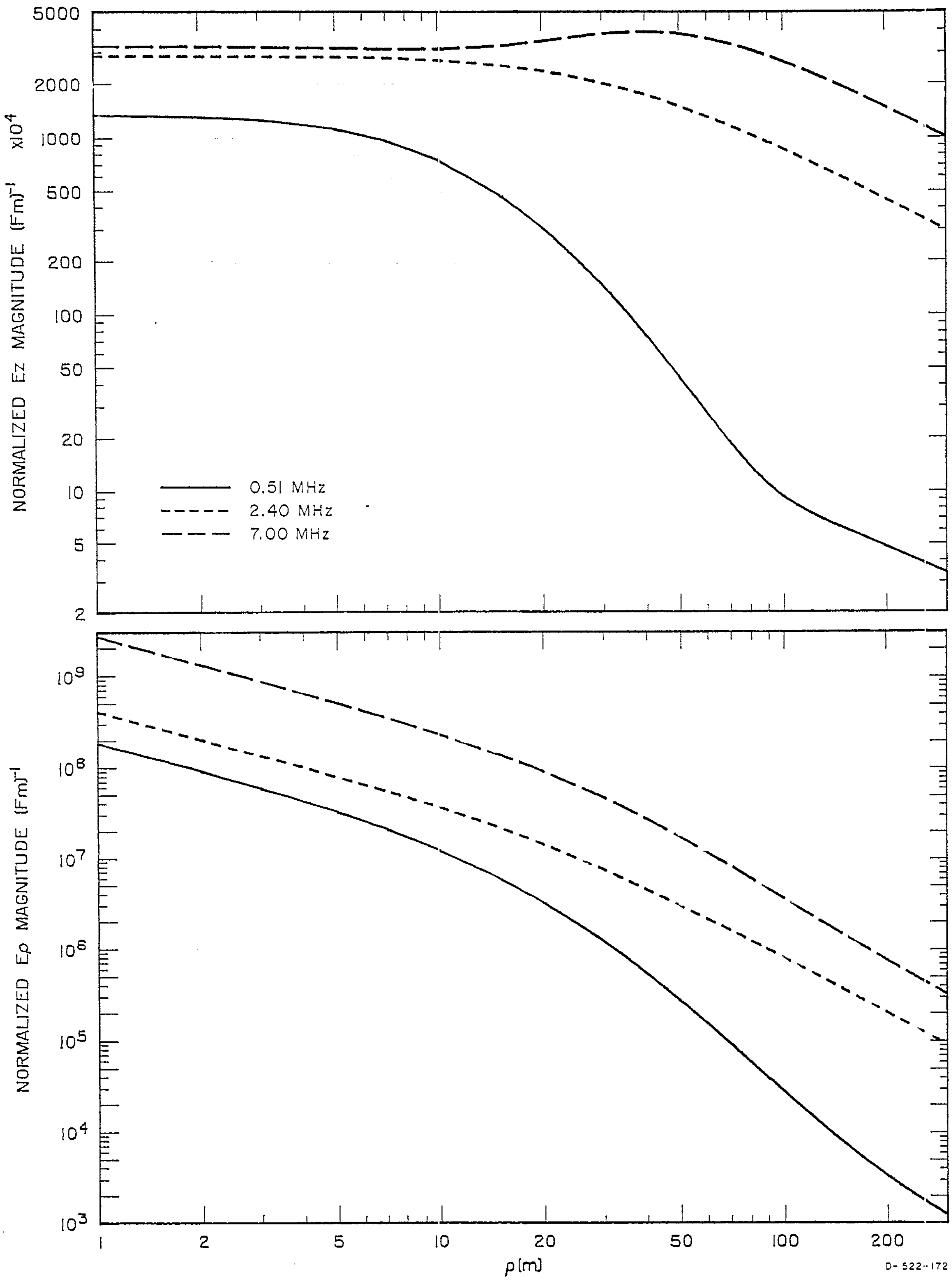

FIG. 3 NORMALIZED ELECTRIC FIELD COMPONENTS
FOR $z = 9.15$ m., $\ell = 33.1$ m.

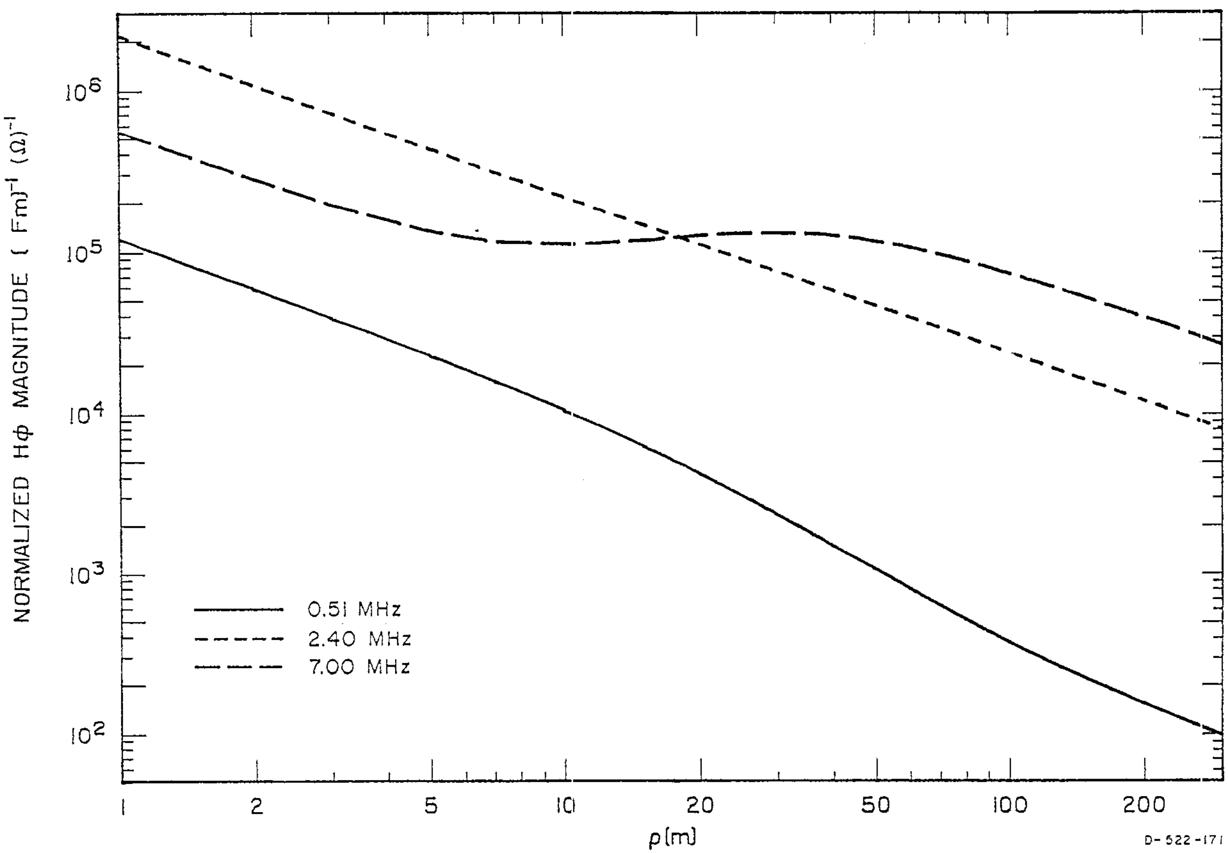

FIG. 4 NORMALIZED MAGNETIC FIELD COMPONENTS
FOR z = 9.15 m., ℓ = 33.1 m.

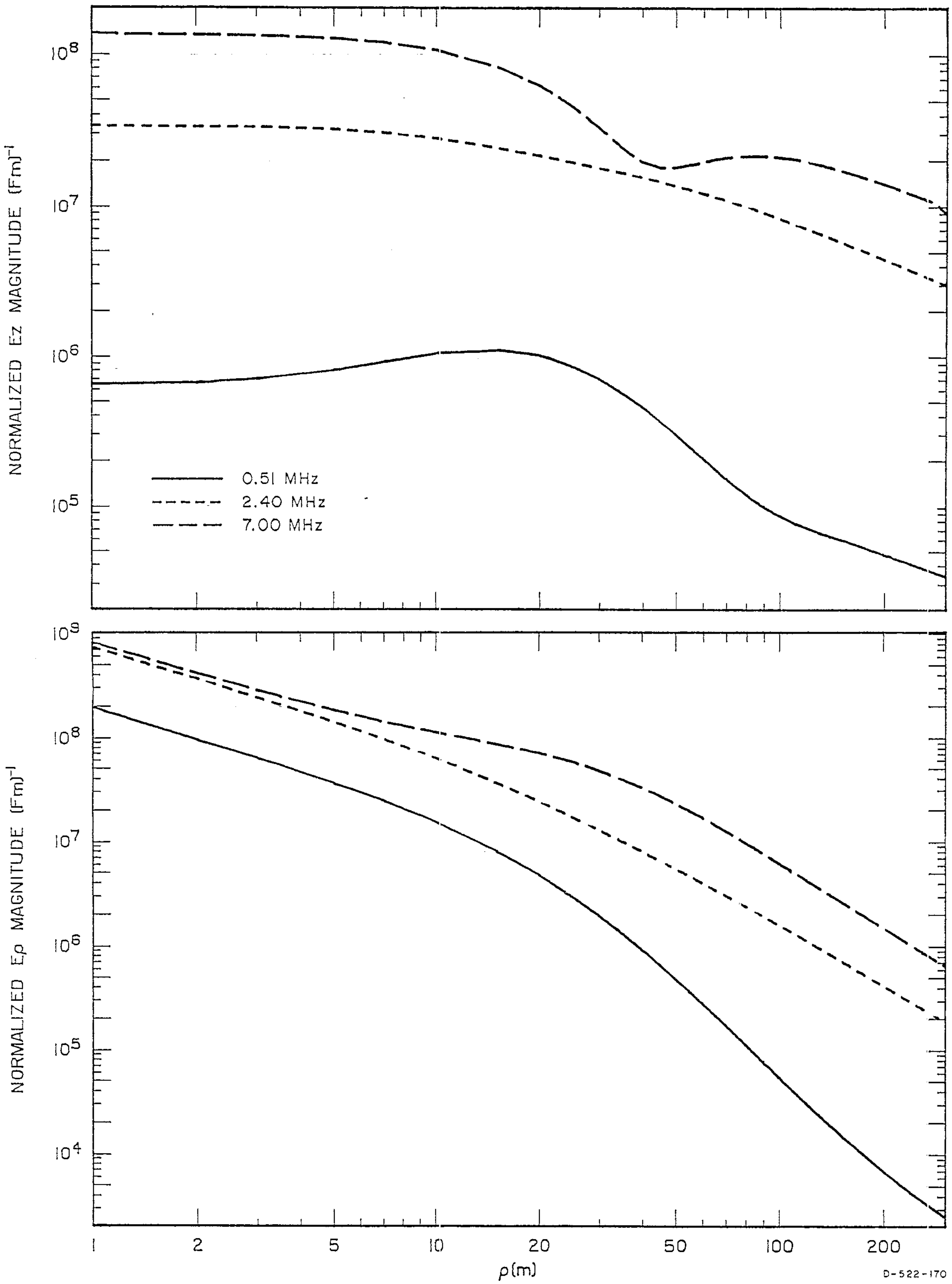

FIG. 5 NORMALIZED ELECTRIC FIELD COMPONENTS
FOR z = 18.3 m., ℓ = 33.1 m.

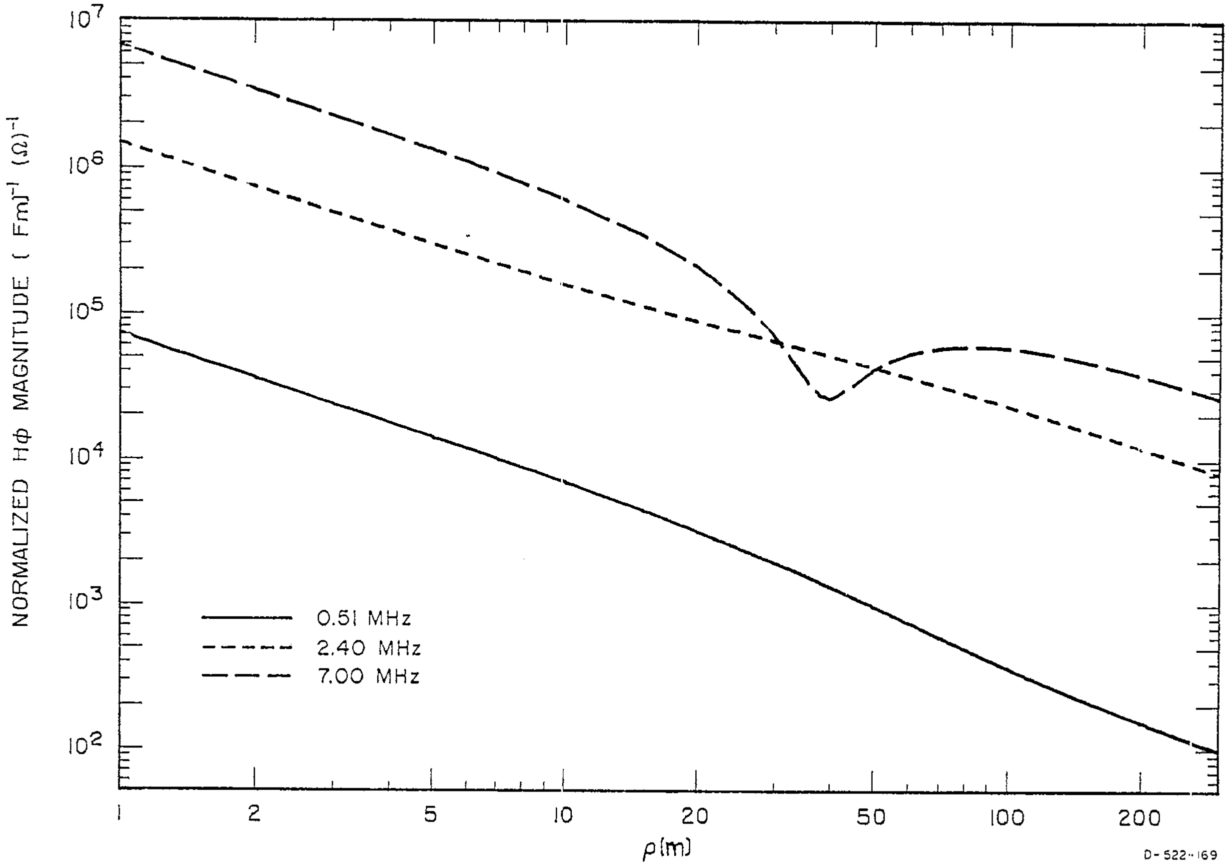

FIG. 6 NORMALIZED MAGNETIC FIELD COMPONENT FOR z = 18.3 m., ℓ = 33.1 m.

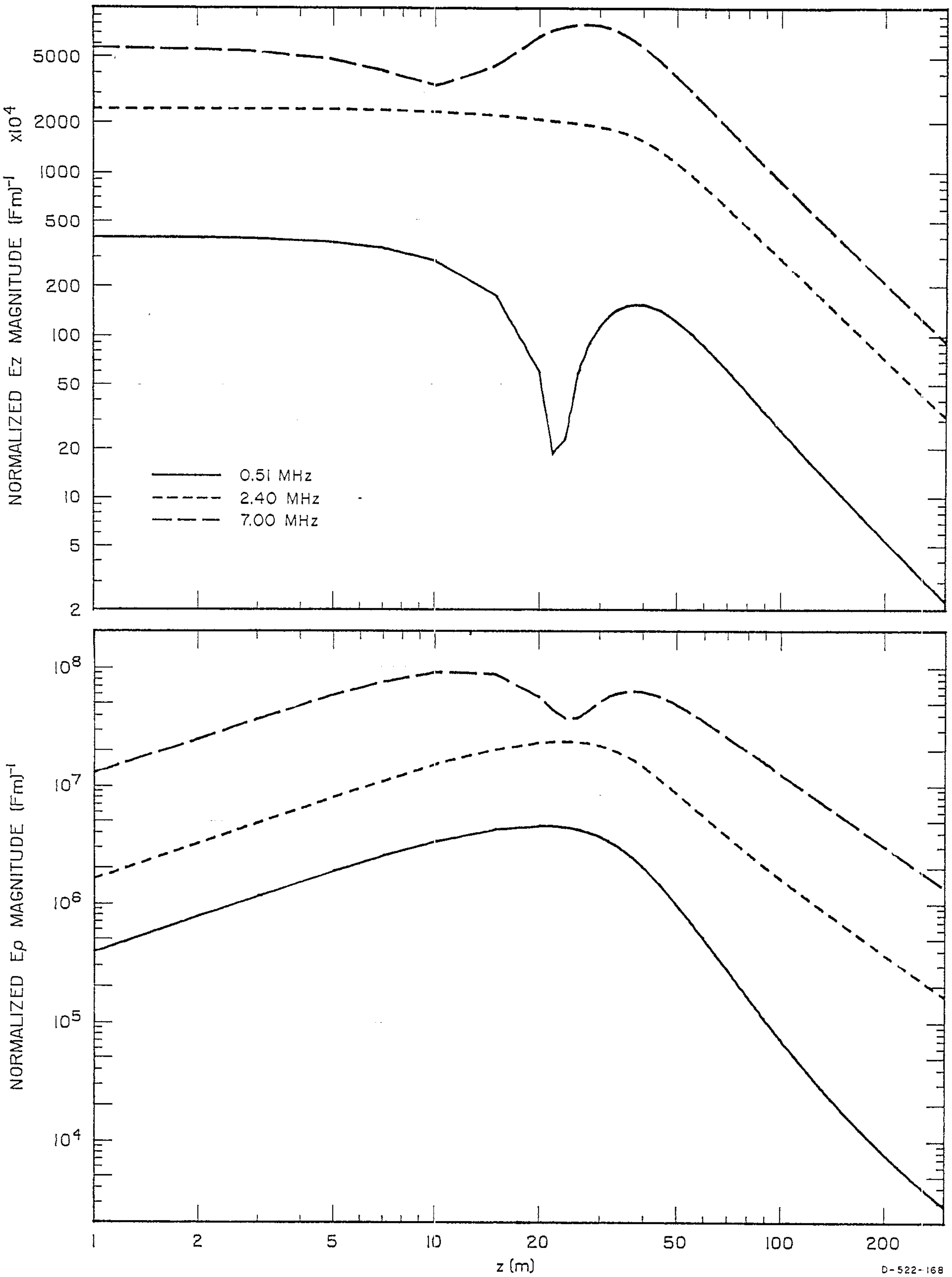

FIG. 7 NORMALIZED ELECTRIC FIELD COMPONENTS FOR ρ = 20.3 m., ℓ = 33.1 m.

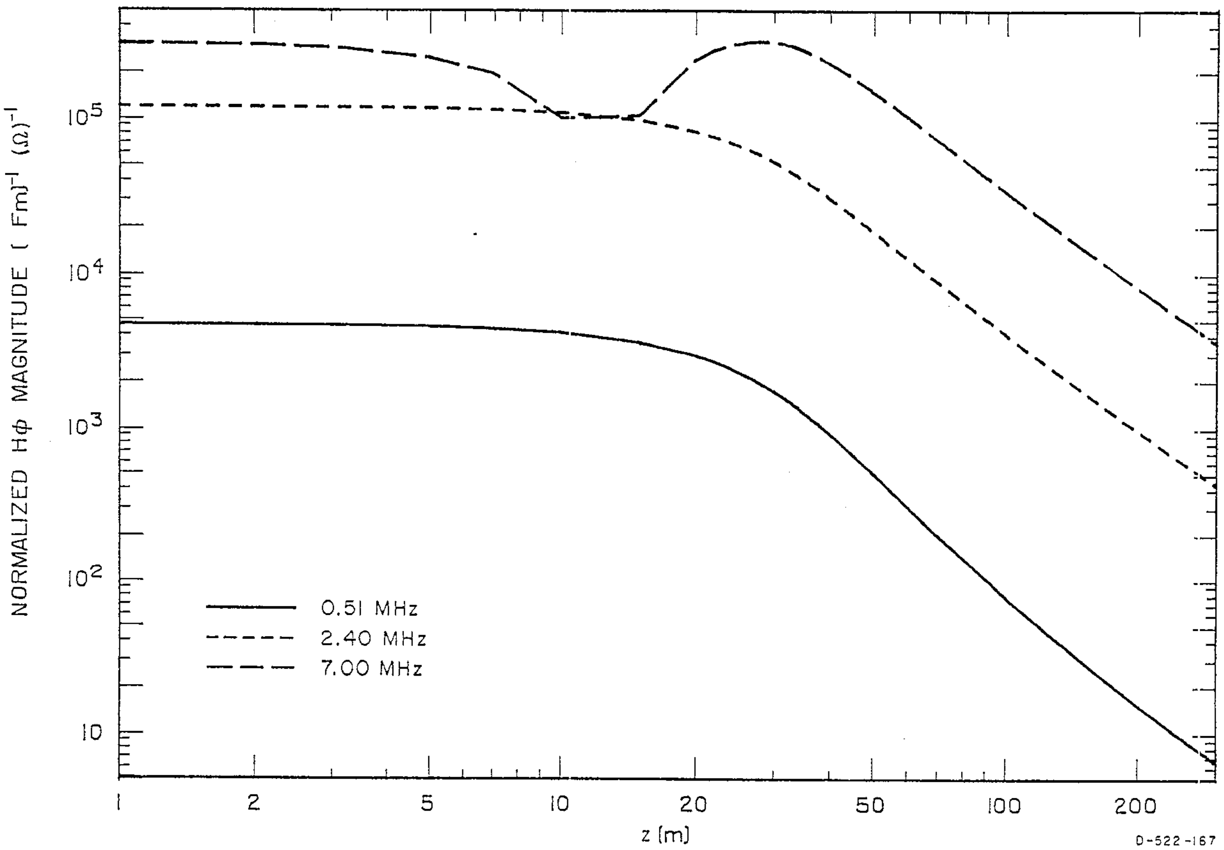

FIG. 8 NORMALIZED MAGNETIC FIELD COMPONENT FOR ρ = 20.3 m., ℓ = 33.1 m.

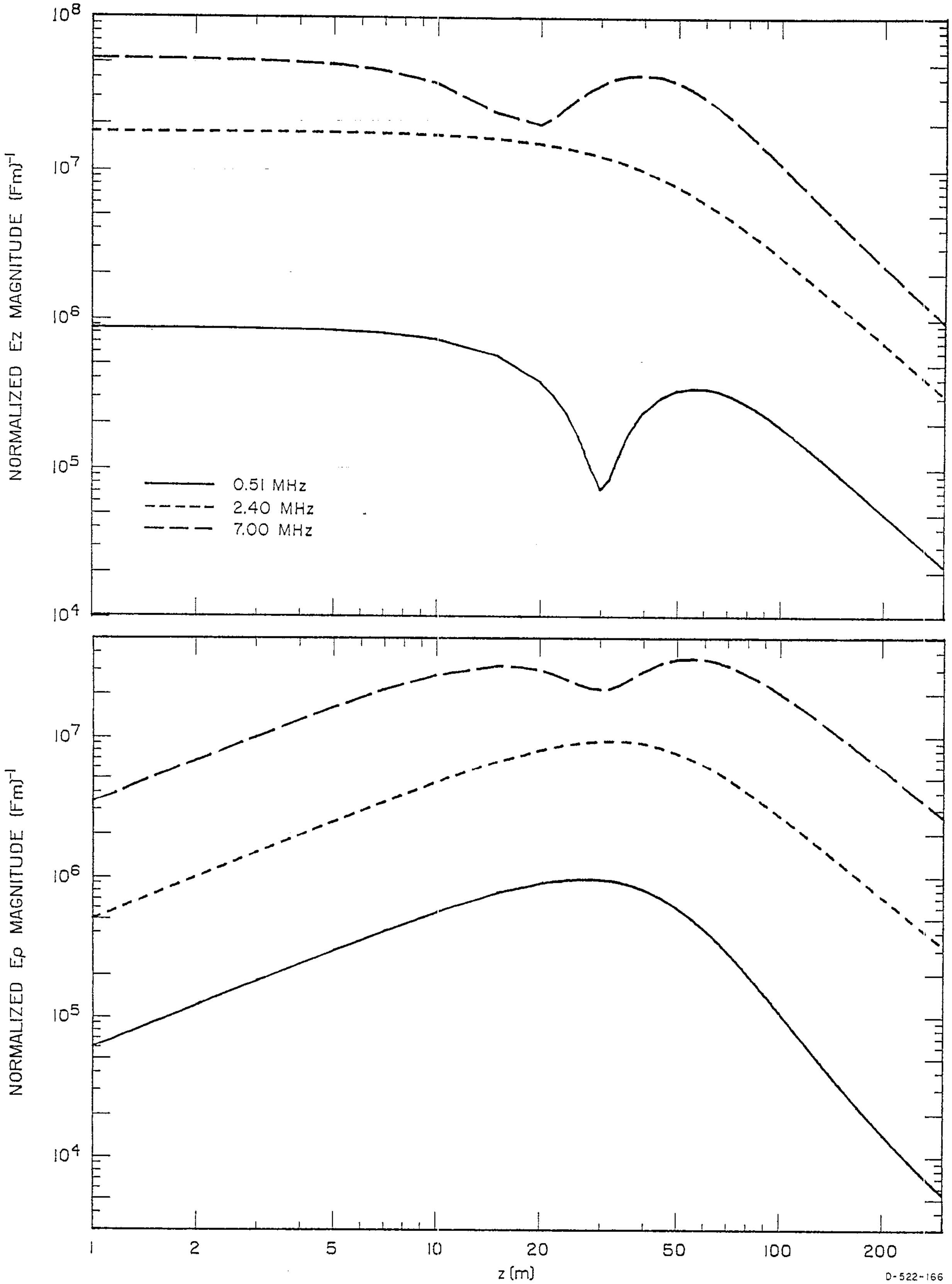

FIG. 9 NORMALIZED ELECTRIC FIELD COMPONENTS FOR ρ = 40.6 m., ℓ = 33.1 m.

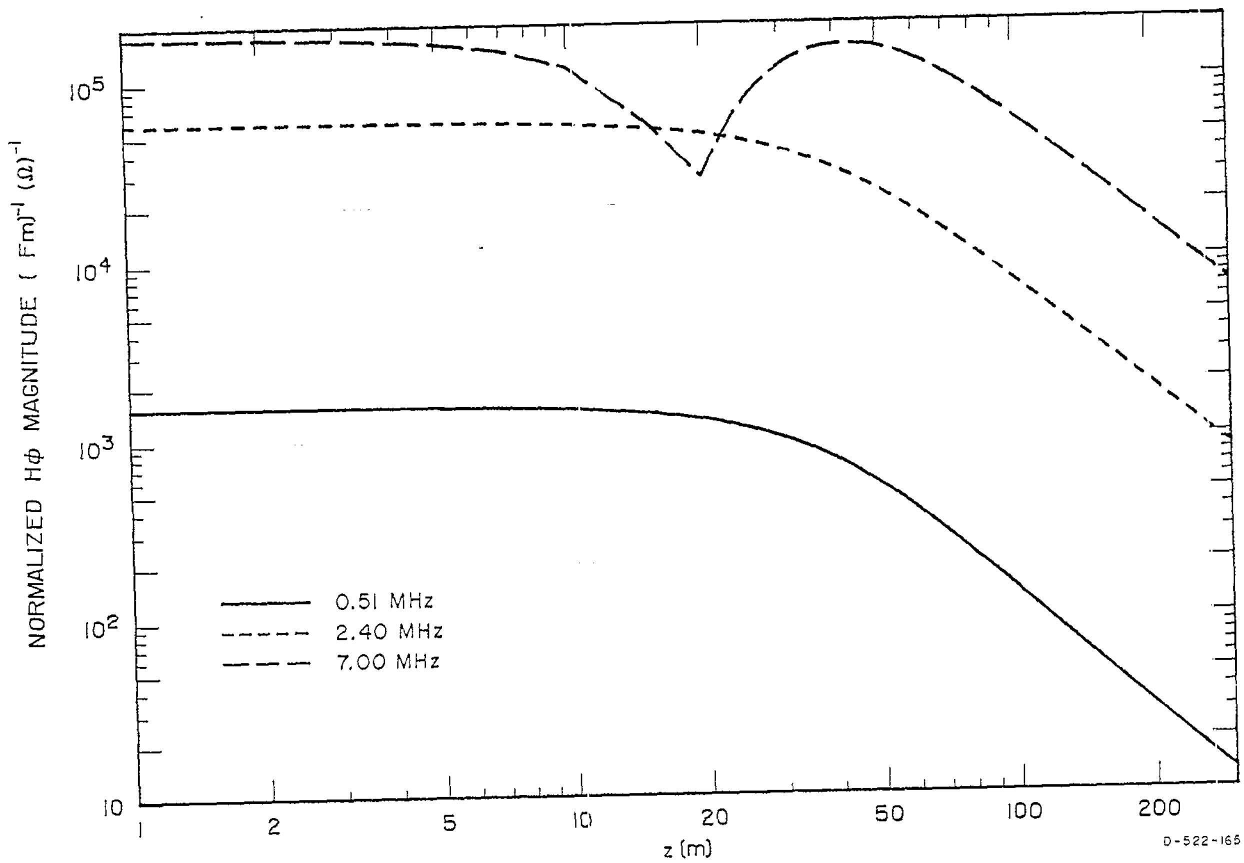

FIG. 10 NORMALIZED MAGNETIC FIELD COMPONENT
FOR ρ = 40.6 m., ℓ = 33.1 m.

V. Discussion

The results for the E_z electric field case at $z = 0$ are shown in the upper graph of figure 2. The variations of E_z with ρ at $f = 0.51$ MHz are listed in table 1.

Table 1

Variation of E_z with ρ	Range of ρ(m)	Zone	
$\sim \rho^{-1}$	$120 < \rho$	Radiation	$(k\rho > 1)$
$\sim \rho^{-2}$	$80 \lesssim \rho \lesssim 120$	Induction	$(k\rho \approx 1)$
$\sim \rho^{-3}$	$50 \lesssim \rho \lesssim 80$	Static	$(k\rho < 1)$
$\sim \rho^{-2}$	$15 \lesssim \rho \lesssim 50$	Transition	$(\rho \lesssim 2\ell)$
$\sim \rho^{-1}$	$\rho < 15$	Uniform current	$(\rho < \ell/2)$

The E_z 2.4-MHz (quarter-wavelength) curve in figure 2 varies as ρ^{-1} in the radiation zone $(k\rho > 1)$. However, the slope approaches zero as $\rho \to 0$, because the antenna supports a quarter-wave current distribution. The 7.0-MHz (three-quarter-wavelength) curve in figure 2 also varies as ρ^{-1} in the radiation zone. There is a minimum at $\rho \approx 10$m caused by the three-quarter-wave current distribution. As in the case of the 0.51-MHz curve, the 7.0-MHz curve varies as ρ^{-1} for $\rho \lesssim 10$m. If the source were an infinitesimally small (point) source, then the E_z component would vary as ρ^{-3} for $0 < \rho \lesssim 60\text{m} \approx 2\ell$, that is, for $k\rho \ll 1$ for all frequencies. However, because of the distributed source, the variation of E_z with ρ for $0 < \rho \lesssim 2\ell$ is slower than the variation in the static region for all three frequencies.

The results for the magnetic field component H_φ are shown in the lower graph of figure 2. The slopes of all three magnetic field curves vary as ρ^{-1} for $\rho \gtrsim 120$m and for $\rho \lesssim 15$m. The slope for $15 < \rho < 120$m is slightly larger for 0.5 MHz, the same for 2.4 MHz, and slightly smaller for 7.0 MHz. If the source were a point source, then the H_φ component would vary as ρ^{-2} for $0 < \rho \lesssim 30$m, that is, for $k\rho \ll 1$ and $\rho \lesssim \ell$. The distributed source causes the variation of H_φ with ρ for $0 < \rho \lesssim \ell$ to be slower than the variation in the induction region $(\rho > 2\ell)$. At distances within one antenna height, both E_z and H_φ vary as ρ^{-1}, as is the case for the radiation zone. However, the phase variations of E_z and H_φ for $\rho < \ell$ are different from those for the radiation region $(\rho > 2\ell)$.

The results for the E_z electric field component for a fixed height of $z = 9.15$m are shown in the upper graph of figure 3. The variations of E_z with ρ for $f = 0.51$ MHz are listed in table 2.

Table 2

Variation of E_z with ρ	Range of ρ(m)	Zone
$\sim \rho^{-1}$	$120 < \rho$	Radiation ($k\rho > 1$)
$\sim \rho^{-2}$	$80 \lesssim \rho \lesssim 120$	Induction ($k\rho \approx 1$)
$\sim \rho^{-3}$	$40 \lesssim \rho \lesssim 80$	Static ($k\rho < 1$)
$\sim \rho$	$15 \lesssim \rho \lesssim 40$	Transition ($\rho \lesssim 2\ell$)
$\sim$ Constant	$\rho < 15$	Uniform current ($\rho < \ell/2$)

As in the case for the 0.51-MHz curve, the slopes of the 2.4- and 7.0-MHz E_z curves in figure 3 vary as ρ^{-1} in the radiation zone and are constant in the uniform current zone. The 2.4-MHz curve is also monotonic, but the 7.0-MHz curve has a peak at $\rho \approx 50$m caused by the current distribution.

The results for the E_ρ electric field component for z = 9.15m are shown in the lower graph of figure 3. The variations of E_z with ρ for f = 0.51 MHz are listed in table 3.

Table 3

Variation of E_ρ with ρ	Range of ρ(m)	Zone
$\sim \rho^{-2}$	$120 < \rho$	Radiation
$\sim \rho^{-3}$	$30 \lesssim \rho \lesssim 120$	Induction static
$\sim \rho^{-2}$	$15 \lesssim \rho \lesssim 30$	Transition
$\sim \rho^{-1}$	$\rho < 15$	Uniform current

As in the case for the 0.51-MHz curve, the slopes of the 2.4- and 7.0-MHz E_ρ curves vary as ρ^{-2} in the radiation zone and are constant in the uniform current zones.

The results for the H_φ magnetic field component for z = 9.15m are shown in figure 4. The slopes of all three curves vary as ρ^{-1} for $\rho \gtrsim 120$m and for $\rho \lesssim 15$m. The slope for $15 < \rho < 120$m is slightly larger for 0.5 MHz, the same for 2.4 MHz, and approximately constant for 7.0 MHz.

In comparing the results in figure 2 for z = 0 with those in figures 3 and 4 for z = 9.15m, several observations can be made. All the curves vary approximately as ρ^{-1} in the radiation field ($\rho > 120$m). The fields increase with increasing frequency in the radiation field. In the transition zone ($\rho \lesssim 30$ m $\approx \ell$), the slope of the fields is always less than that in the static zone. In the uniform current region, the slope of the field components is always less than or equal to the slope in the radiation zone. The two magnetic field graphs are quite similar in slope and magnitude, with the exception of the 7.0-MHz curve in figure 4, which is reduced approximately one order of magnitude for $\rho < 30$m.

The results for the E_z electric field component for a fixed height of $z = 18.3$m are shown in the upper graph of figure 5. The variations of E_z with ρ for $f = 0.51$ MHz are listed in table 4.

Table 4

Variation of E_z with ρ	Range of ρ(m)	Zone
$\sim \rho^{-1}$	$120 < \rho$	Radiation
$\sim \rho^{-2}$	$30 \lesssim \rho \lesssim 120$	Induction, Static
$\sim \rho^{-1}$	$15 \lesssim \rho \lesssim 30$	Transition
Constant	$\rho < 15$	Uniform current

As in the case for the 0.51-MHz curve, the slopes of the 2.4- and 7.0-MHz E_z curves in figure 5 vary as ρ^{-1} in the radiation zone and are constant in the uniform current zone. The 7.0-MHz curve has a minimum at $\rho \approx 50$m, and the 0.51-MHz curve has a slight maximum at $\rho = 15$m. For the uniform current zone, the value of the E_z 0.51-MHz curve in figure 5 is about 0.1 that in figure 3. The 7.0-MHz curve has a minimum around $\rho = 50$m, while it has a maximum in figure 3; for the uniform current zone, the value of the 7.0-MHz curve for E_z in figure 5 is that in figure 3. Otherwise the magnitudes and slopes are about the same.

The results for the E_ρ electric field component for $z = 18.3$m are shown in the lower graph of figure 5. The variations of E_ρ with ρ for $f = 0.51$ MHz are essentially the same as those of the 0.51-MHz curve for E_ρ in figure 3 and are listed in table 3. The results for the H_φ magnetic field component for $z = 18.3$m are shown in figure 6. The 0.51- and 2.4-MHz curves are essentially the same as those in figure 4. The 7.0-MHz curve is the same in the radiation zone and is ten times larger in magnitude with the same ρ^{-1} variation in the uniform current zone. However, in this case there is a distinct minimum in the 7.0-MHz curve at $\rho \approx 40$m, which does not exist in figure 4.

The results for the E_z field variations with height z for a fixed radial distance $\rho = 20.3$m are shown in the upper graph of figure 7. The E_z field is constant for $z \lesssim 15\text{m} \approx \ell/2$ and varies as z^{-2} for $z \gtrsim 70\text{m} \approx 2\ell$. The 0.51-MHz curve has a distinct minimum at $z \approx 20\text{m} \approx \rho$, and the 7.0-MHz curve has a maximum at $z \approx 30\text{m} \approx \ell$. The corresponding results for the E_ρ field variations with z for $\rho = 20.3$m are shown in the lower graph of figure 7. The E_ρ field varies as z^{+1} for $z < 15\text{m} \approx \ell/2$. The 0.51- and 2.4-MHz curves reach their maximum at $z \approx 30\text{m} \approx \ell$, but the 7.0-MHz curve has a local minimum there. The 2.4- and 7.0-MHz curves vary as z^{-2} for $z > 70\text{m} \approx 2\ell$, but the 0.51-MHz curve has a slightly larger slope.

The results for the H_φ field variations with z for $\rho = 20.3$m are shown in figure 8. The slopes of the H_φ curves are approximately the same as those of E_z in figure 7, except that there is no minimum in the H_φ-MHz curve at $z = \rho$. Consequently, the impedance ratio E_z/H_φ at the same frequency is almost constant in each zone, except for the 7.0-MHz case for $z \approx 1$.

The results for the E_z and E_ρ variations with z for $\rho = 40.6$m, shown in figure 9, are essentially the same as those in figure 7. The magnitudes are reduced slightly, since the observation points are further away from the source. Similarly, the H_φ variations with z for $\rho = 40.6$m, shown in figure 10, are essentially the same as those in figure 8. The minimum in the 7.0-MHz curve is slightly sharper in figure 10, and again the magnitudes are reduced slightly.

VI. Conclusions.

The important observations from the graphs and discussion are summarized.

1. The E_z and H_φ vary as ρ^{-1} in the radiation zone for $\rho \gtrsim 120\text{m} \approx 4\ell$ for $z = 0$, 9.15, and 18.3m and for f = 0.51, 2.4, and 7.0 MHz. The E_ρ varies as ρ^{-2} in this radiation zone for z = 9.15 and 18.3m. Thus, for these heights and frequencies, the fields in the radiation zone behave as they would from a point source.

2. The E_z for z = 0 varies as ρ^{-2} in the induction zone ($80 \lesssim \rho \lesssim 120$m) and as ρ^{-3} in the static zone ($50 \lesssim \rho \lesssim 80$m) for f = 0.51 MHz, again as in the case of a point source. However, the E_z varies as ρ^{-2} in the transition region ($15 \lesssim \rho \lesssim 50$m) and as ρ^{-1} in the uniform current region ($\rho \lesssim 15\text{m} \approx \ell/2$). The E_z for f = 2.4 and 7.0 MHz never varies faster than ρ^{-1}. Thus, for these two higher frequencies, there are no induction and static zones, because these zones occur so close to the antenna that the distributed current changes the variation with distance from that of a point source.

3. With minor exceptions, the H_φ varies as ρ^{-1} for $\rho \gtrsim 4\ell$ for the three heights and for the three frequencies.

4. The E_z and H_φ are constant near the earth ($0 < z \lesssim \ell/2$) for $\rho = 20.3$ and 40.6m for f = 0.51, 2.4, and 7.0 MHz. The E_z and H_φ decrease as z^{-2} for $z \gtrsim \ell$. Thus the impedance E_z/H_φ is a constant within each zone (except for a few special cases mentioned in the discussion).

5. The E_ρ increases with height as z^{+1}, reaches a peak around $z \approx \ell$, and decreases as z^{-2} for $z \gtrsim 2\ell$, for both radial distances and for all three frequencies.

Finally, the distributed source must be considered to determine accurately the electromagnetic field components from an antenna for $\rho < 2\ell$; however, a point source gives reasonably accurate results for $\rho > 2\ell$. The effect of the distributed source is to cause the components to vary with ρ and z considerably slower than they would from a point source.

References

E. C. Jordan, Electromagnetic Waves and Radiating Systems (Prentice-Hall, Inc., New York, N.Y., 1950).

R. W. P. King, The Theory of Linear Antennas (Harvard University Press, Cambridge, Massachusetts, 1956).

R. W. P. King and T. T. Wu, "Currents, Charges, and Near Fields of Cylindrical Antennas," J. Res. NBS, Radio Science, Vol. 69D, No. 3, pp. 429-446 (1965).

Y. T. Lo, "A Note on the Cylindrical Antenna of Noncircular Cross-Section," J. Appl. Phys., Vol. 24, Part 2, No. 10, pp. 1338-1339 (1953).